# Monte Carlo simulations of the fcc kagome lattice: Competition between triangular frustration and cubic anisotropy

M. D. LeBlanc, M. L. Plumer, and J. P. Whitehead

*Department of Physics and Physical Oceanography, Memorial University of Newfoundland, St. John's, Newfoundland, Canada A1B 3X7*

B. W. Southern

*Department of Physics and Astronomy, University of Manitoba, Winnipeg, Manitoba, Canada R3T 2N2*

The impact of local cubic anisotropy on the magnetic states of the Heisenberg model on the fcc kagome lattice are examined through classical Monte Carlo simulations. Previous simulations revealed that the macroscopic degeneracy of the two-dimensional (2D) kagome exchange-coupled co-planar spin system partially persists in the 3D case of ABC stacked layers giving rise to a discontinuous phase transition. Local cubic anisotropy is shown to remove this degeneracy by re-orienting the spins out of the co-planar configuration. In addition, the re-oriented states are shown to carry a uniform magnetic moment. Simulation results indicate that the effect of anisotropy is to transform the first-order phase transition to a continuous one. These results are relevant to Ir-Mn alloys which have been widely used by the magnetic storage industry in thin-film form as the antiferromagnetic pinning layer in spin valves.

PACS number(s): 75.10.Hk, 75.30.Gw, 75.40.Mg

## I. INTRODUCTION

The macroscopic degeneracy associated with magnetic dipoles on the two-dimensional (2D) kagome lattice composed of corner-sharing triangles, with four near-neighbor (NN) exchange interactions, continues to generate new physics after twenty years of study.[1–3] The main focus of these works has been associated with ultralow temperature and quantum effects. Quasi-3D experimental manifestations have been limited to systems with weakly coupled kagome layers or distorted hyperkagome lattice structures.[2,4] Studies of a true 3D version of the kagome structure composed of ABC stacked kagome layers, with four in-plane and four out-of-plane identical antiferromagnetic (AF) NN exchange interactions which we call the fcc kagome lattice, depicted in Figs. 1 and 2, have recently demonstrated long-range magnetic order at temperatures comparable to the exchange interaction.[5,6]

For continuous spin models on the 2D kagome lattice with NN exchange interactions, the ground state is highly degenerate with a net zero magnetic moment for each triangle giving rise to $120°$ spin structures in either $q = 0$ or $\sqrt{3} \times \sqrt{3}$ co-planar forms.[1] The $120°$ spin structure can be thought of as three interpenetrating ferromagnetic sublattices. In addition to the usual continuous degrees of freedom associated with $XY$ and Heisenberg models, the $q = 0$ spin structure on the 2D kagome lattice allows for the interchange of sub-lattice spins with its neighbor along a row with no change in energy. Unlike the triangular lattice AF, there is no correlation between the chiralities of adjacent triangles.[7] In the 3D fcc kagome case, the $q = 0$ structure is selected and two sublattice spins within a plane defined by the eight NN exchange interactions can be reoriented with no cost in energy.[6,8]

Interest in the fcc kagome lattice has been driven not only by it being a unique realization of this type of frustration in three dimensions but also due to its connection with thin-film magnetic technology through IrMn$_3$, which is commonly used as the exchange pinning layer in spin valves.[9–11] This and sister compounds RhMn$_3$ and PtMn$_3$ have the fcc CuAu$_3$ crystal structure[12] where magnetic Mn ions reside on the cube faces and the nonmagnetic (Ir) ions site at the cube corners. The magnetic ions can thus be viewed as being on ABC stacked (111) kagome planes, where each site has eight NNs (four in-plane, two to the plane above, and two to the plane below) as shown in Fig. 1 of Ref. 6. Bulk IrMn$_3$ was shown to have long-range magnetic order below $T_N \approx 960$ K,[13] referred to as the "T1" structure, which is the 3D manifestion of the $120°$ $q = 0$ spin structure.[6] Similar magnetic order is also found in RhMn$_3$ and PtMn$_3$. In thin-film applications, the (111) plane is perpendicular to the film plane. It is of interest to note that the 3D $q = 0$ structure remains favored in the presence of 6 ferromagnetic second-NN exchange interactions, 16 AF third-NN exchange and 12 ferromagnetic fourth-NN exchange interactions calculated for IrMn$_3$.[5]

Agreement on the fundamental mechanism responsible for exchange bias in Ir-Mn thin films and other materials remains elusive.[14] It is believed that frustration of some sort at the interface between the AF and ferromagnet is essential.[15] It is clear that there needs to be a pinned ferromagnetic component within the first few layers of the AF. Some studies also suggest that exchange bias is enhanced if this moment is perpendicular to the plane of the film.[16,17] An essential requirement for technological applications is that the AF layer magnetically orders well above room temperature.

Szunyogh *et al.*[5] used symmetry arguments supported by electronic structure calculations to demonstrate the importance of an effective local-axis cubic anisotropy term in the spin Hamiltonian for IrMn$_3$ (see Fig. 2). Its value is estimated to be about 10% of the NN exchange strength and gives a preference for the sublattice moments to be directed out of a co-planar configuration and to be along the three $\langle 100 \rangle$ axes. The projection of the spins in the {111} plane maintains the $120°$ structure.

We examine here effects of adding cubic anisotropy to the NN Heisenberg fcc kagome lattice AF through a series of
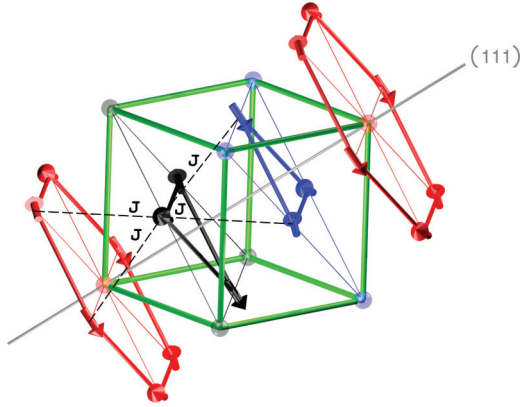
FIG. 1. (Color online) The fcc kagome lattice with magnetic Mn ions on cube faces forming stacked 2D kagome layers along the (111) axis. Nonmagnetic Ir ions are at the corners. The four interlayer exchange interactions (J) are indicated.

extensive Monte Carlo (MC) simulations. Previous MC results of Heisenberg and *XY* models on this lattice which included only exchange effects revealed the spin degeneracies in three dimensions and supported the notion that the discontinuous phase transition is of the order-by-disorder type.[6] In the present work, an analytic calculation of the ground state reveals an out-of-plane rotation of the sublattice spins driven by the anisotropy as well as a concomitant net magnetic moment perpendicular to the plane. The effect of anisotropy in removing certain degeneracies is determined. The impact of anisotropy on the Néel temperature and various thermodynamic properties is studied. In addition, results from energy histograms and fourth-order cumulants[18] are used to argue that the transition changes from discontinuous to continuous as a consequence of anisotropy reducing spin degeneracies.

This paper is organized as follows. In Sec. II, the Heisenberg model on a 3D kagome fcc lattice is described with a focus on the effect of cubic anisotropy. In Sec. III, analytical calculations are presented for the zero-temperature ground states. In Sec. IV, MC simulation results are shown that describe the effect of the anisotropy on the critical temperature behavior. This section also analyzes the order of the phase transition in comparison to the model without anisotropy. We discuss the results and extensions for future work in Sec. V.
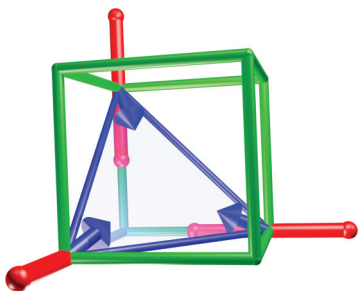


FIG. 2. (Color online) Schematic showing a 120° ground-state spin structure (blue arrows) in the cubic (111) plane, along with the local [100] anisotropy axis directions (red rods). The cube shown has sides of length $a/2$, where $a$ is the lattice constant of the fcc unit cell.

## II. MODEL

We consider a 3D lattice that consists of $L$ layers of $L \times L$ spins per kagome (111) plane, ABC stacked as shown in Fig. 1. MC simulations were done on this model using lattice sizes $L = 18, 24, 30$, and 36. All the simulations were performed using the Metropolis algorithm. This method gave satisfactory results even down to the lowest relevant temperatures. Typically between $10^5$ and $10^7$ Monte Carlo steps (MCSs) were used with an initial 10% discard rate for equilibration. The interactions include NN Heisenberg exchange, and the effective local cubic anisotropy developed by Szunyogh *et al.*,[5] as described by the Hamiltonian

$$\mathcal{H} = J \sum_{\langle i,j \rangle} \mathbf{S}_i \cdot \mathbf{S}_j - K \sum_{\gamma} \sum_{k \subset \gamma} (\mathbf{S}_k \cdot \mathbf{n}_\gamma)^2, \qquad (1)$$

where $i, j$ are summed over all the $N = \frac{3}{4}L^3$ spins of the entire lattice, $J \equiv 1$ is the antiferromagnetic coupling to the four in-plane and four out-of-plane NN spins, and the anisotropy $K > 0$ is varied over a wide range of values. Here, $\gamma$ represents sublattice 1, 2, and 3 and $k$ is summed over the $\frac{N}{3} = \frac{1}{3}(\frac{3}{4}L^3)$ spins of sublattice $\gamma$, $\mathbf{S}_i$ are unit spin vectors at each site, and $\mathbf{n}_\gamma$ are unit vectors in the cube axes directions, $\mathbf{n}_1 = \hat{\mathbf{x}}$, $\mathbf{n}_2 = \hat{\mathbf{y}}$, and $\mathbf{n}_3 = \hat{\mathbf{z}}$, as in Fig. 2. Electronic structure calculations[5] have been used to estimate $K \approx 0.1$ in the case of IrMn$_3$ but we consider a wide range of anisotropy values.

There are two order parameters calculated for this model. The sublattice magnetization is defined as

$$M_t = \frac{1}{N} \left\langle \sum_{\gamma} \left| \sum_{k \subset \gamma} \mathbf{S}_k \right| \right\rangle. \qquad (2)$$

Angular brackets denote thermal averaging over MC states. A similar order parameter was also used in the case[6] of $K = 0$ to characterize the ground-state spin configuration. With the addition of anisotropy, the ferromagnetic magnetization vector becomes nonzero and is defined as

$$M_f = \frac{1}{N} \left| \left\langle \sum_i \mathbf{S}_i \right\rangle \right|. \qquad (3)$$

It is zero for all temperatures when $K = 0$ and in the paramagnetic state with $K \neq 0$. Its zero-temperature value can be calculated analytically, as shown below.

## III. GROUND STATE

Analysis of the effect of the anisotropy is made convenient by defining $\alpha$ as the cosine of the angle between each sublattice spin and its anisotropy axis [$\alpha = \cos(\mathbf{S}_i \cdot n_i)$] and $\beta$ the cosine of the angle with respect to the other anisotropy axes [$\beta = \cos(\mathbf{S}_i \cdot n_j)$, $i \neq j$]. As such, each spin will have direction cosines of the general form 1:$(\pm\alpha, \pm\beta, \pm\beta)$, 2:$(\pm\beta, \pm\alpha, \pm\beta)$, and 3:$(\pm\beta, \pm\beta, \pm\alpha)$. When $K = 0$, this gives specific planar configurations of the system's many degenerate ground states.

With the addition of a finite anisotropy, the continuous degeneracy is removed, as the spins now have a preferential direction. There are eight possible ground states when this anisotropy is added to the system, corresponding to the four possible (111) planes with two configurations related to spins

being lifted out of either side of each plane. These can be enumerated as

$$\pm(111) \rightarrow \pm[\boldsymbol{S}_1 = (\alpha, -\beta, -\beta), \boldsymbol{S}_2 = (-\beta, \alpha, -\beta), \boldsymbol{S}_3 = (-\beta, -\beta, \alpha)], \tag{4}$$

$$\pm(\bar{1}11) \rightarrow \pm[\boldsymbol{S}_1 = (-\alpha, -\beta, -\beta), \boldsymbol{S}_2 = (\beta, \alpha, -\beta), \boldsymbol{S}_3 = (\beta, -\beta, \alpha)], \tag{5}$$

$$\pm(1\bar{1}1) \rightarrow \pm[\boldsymbol{S}_1 = (\alpha, \beta, -\beta), \boldsymbol{S}_2 = (-\beta, -\alpha, -\beta), \boldsymbol{S}_3 = (-\beta, \beta, \alpha)], \tag{6}$$

$$\pm(11\bar{1}) \rightarrow \pm[\boldsymbol{S}_1 = (\alpha, -\beta, \beta), \boldsymbol{S}_2 = (-\beta, \alpha, \beta), \boldsymbol{S}_3 = (-\beta, -\beta, -\alpha)]. \tag{7}$$

Since each spin is a unit vector,

$$\boldsymbol{S}_i \cdot \boldsymbol{S}_i = 1 = \alpha^2 + 2\beta^2. \tag{8}$$

The system energy per spin is given by

$$E = \tfrac{4}{3}J(\boldsymbol{S}_1 \cdot \boldsymbol{S}_2 + \boldsymbol{S}_2 \cdot \boldsymbol{S}_3 + \boldsymbol{S}_3 \cdot \boldsymbol{S}_1)$$
$$- \tfrac{1}{3}K[(\boldsymbol{S}_1 \cdot \boldsymbol{n}_1)^2 + (\boldsymbol{S}_2 \cdot \boldsymbol{n}_2)^2 + (\boldsymbol{S}_3 \cdot \boldsymbol{n}_3)^2] \tag{9}$$

with the energy in the ground state given by

$$E = 4(\beta^2 - 2\alpha\beta) - K\alpha^2. \tag{10}$$

Finding the energy minimum and solving for $\alpha$ gives

$$\alpha = \sqrt{1/2 + 1/2\sqrt{1 - 1/[1 + (K+2)^2/32]}} \tag{11}$$

and [from Eq. (8)]

$$\beta = \sqrt{\frac{1-\alpha^2}{2}} \tag{12}$$

using the positive values of the square roots to give physical solutions. When $K = 0$, $\alpha = 2/\sqrt{6}$ and $\beta = 1/\sqrt{6}$ which defines spins in the co-planar $120°$ spin structure.

For low values of $K$, an expansion can be made which gives an energy per magnetic site in the ground state of $E \simeq -2 - 2K/3$. The degeneracy that corresponded to interchanging sublattice spins in a plane at zero anisotropy will now have an energy cost of $K/(3L)$, thus removing the degeneracy up to order $K$.

When $K = 0$, the spins are in one of many degenerate coplanar ground states subject to the requirement that the interspin angle on a triangle be $120°$. This angle can be calculated using $\boldsymbol{S}_i \cdot \boldsymbol{S}_j = \beta^2 - 2\alpha\beta$ for any $i \neq j$ with the analysis above for finite $K$. The results in Fig. 3 show how the
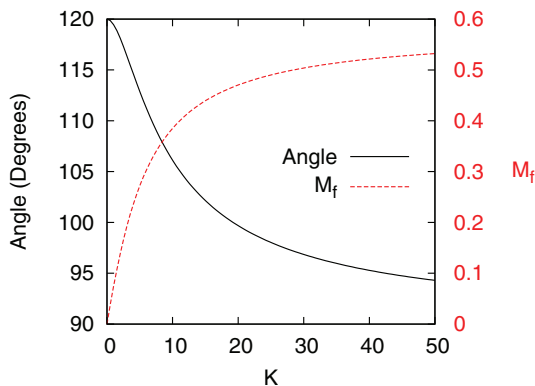
addition of anisotropy modifies the $120°$ spin configuration. In the limit of very large $K$, the angle reaches $90°$ where the spins are pointing along the anisotropy (cube axes) directions.

For any nonzero anisotropy the spins are no longer coplanar and have a net moment directed out of the (111) plane, given by

$$\boldsymbol{M}_f = \boldsymbol{S}_1 + \boldsymbol{S}_2 + \boldsymbol{S}_3$$
$$= [\pm(\alpha - 2\beta), \pm(\alpha - 2\beta), \pm(\alpha - 2\beta)] \tag{13}$$

with its norm equal to $(\alpha - 2\beta)/\sqrt{3}$. The magnetization as a function of $K$ is shown in Fig. 3, where in the limit of large $K$, $M \rightarrow \frac{1}{\sqrt{3}}$.

## IV. SIMULATION RESULTS

Our previous MC simulation results for the $K = 0$ Heisenberg model on the fcc kagome lattice[6] demonstrated the onset of long-range $q = 0$ spin order at $T_N = 0.476J$. Degeneracies were evident by examining the total order parameter $M_t$ in cooling runs, where complete saturation, $M_t \rightarrow 1$ at $T = 0$, does not occur due to sublattice spin switching. In the ground state, any finite amount of anisotropy will lock the spins to a particular (111) plane, thus eliminating the degeneracy associated with the relative orientation of planes of spins.

Figure 4 shows results at $L = 24$ for the total order parameter $M_t$ as a function of temperature in cooling runs for values of $K$ between 0 and 0.06. At each value of $K$, the results of only one run are shown. At values of $K = 0.01$ and 0.04 there is a noticeable impact on removing the degeneracy



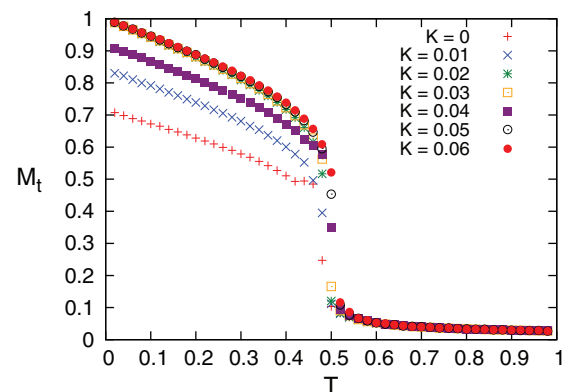FIG. 3. (Color online) Interspin angle and magnetic moment at zero temperature vs anisotropy strength.



FIG. 4. (Color online) Sublattice magnetization order parameter vs temperature for small values of $K$ from simulations with $L = 24$.
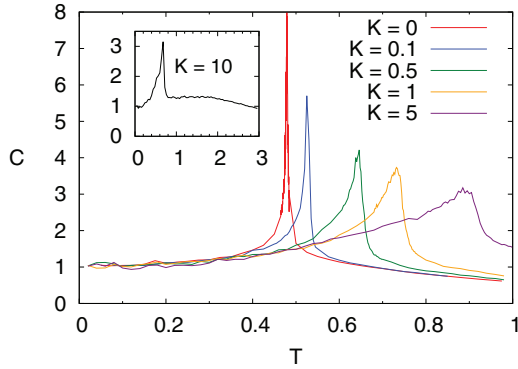
FIG. 5. (Color online) Specific heat vs temperature used to locate $T_N$ for the values of $K$ indicated from simulations with $L = 24$. Inset shows results for $K = 10$ and the expected broad peak at $T \simeq K/6$ due to short-range order.



FIG. 7. (Color online) Simulation results with $L = 24$ for the ferromagnetic magnetization vs temperature for the values of $K$ indicated.

compared to the $K = 0$ results. At $K = 0.03$, 0.05, and 0.06, the system fully saturates. The particular degenerate spin configuration that the system locks into upon cooling below $T_N$ is largely random and the impact of K on reducing the degeneracy is dependent upon its value relative to thermal fluctuations as well as the system size and number of MCSs. For $K$ larger than $\simeq 0.06$, this is no longer the case (for the set of simulation conditions used in this example) and the sublattice magnetization order parameter always tends toward unity as $T = 0$ is approached. This result, together with the analysis of the ground state, is suggestive that any nonzero value of $K$ eliminates the degeneracy that is associated with the NN Heisenberg model on a kagome lattice.

The impact of anisotropy on the transition temperature $T_N$ can be estimated through the location of the specific-heat peak, as shown in Fig. 5 for $K = 0$, 0.1, 0.5, 1, 5, and 10. Note that for large $K$ the system acts primarily under the influence of the single-site uniaxial anisotropy. In this case, a broad maximum in the specific heat is expected[19] at $T \simeq K/6$ due to the onset of short-range correlations well above $T_N$. Such a maximum is seen in the inset of Fig. 5 for $K = 10$.

Figure 6 summarizes the results of estimating $T_N$ from simulations of the specific heat for a wide range of $K$ values. For small and moderate values of $K$ it is seen that $T_N$ increases to a maximum of about 0.9 $J$ at $K \simeq 5$, followed by a
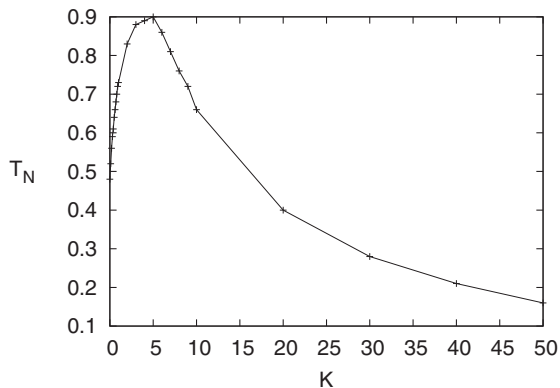


FIG. 6. Néel temperature $T_N$ vs the anisotropy strength $K$ estimated from the specific-heat peaks from simulations with $L = 24$.
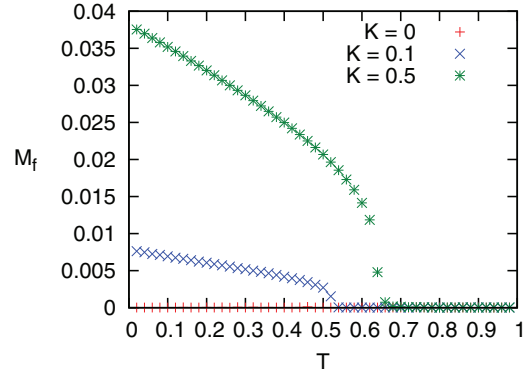
monotonic decrease up to the largest anisotropy value ($K = 50$) examined. In the limit of infinite anisotropy, all NN spins are perpendicular to each other and the interspin exchange interaction would thus be reduced to zero, eliminating long-range order.

Figure 7 shows the total magnetization $M_f$ vs temperature at $K = 0$, 0.1, and 0.5. In the absence of anisotropy, the simulated $M_f$ is zero for all $T$, as expected from the ground-state calculations. Its temperature dependence for the nonzero values of $K$ is similar to the order-parameter results of Fig. 4. The values of $M_f$ extrapolated from these data at $T = 0$ agrees with those expected from the analytic analysis of Sec. III.

In the absence of anisotropy, the Heisenberg fcc kagome lattice has a phase transition that appears to be weakly first order, possibly driven by an order-by-disorder phenomenon. Evidence in support of these ideas was found in MC simulation results of energy histograms and the Binder energy cumulant.[6] The addition of anisotropy removes the usual kagome-type degeneracies and it is believed that this leads to a continuous transition, as would occur within mean-field theory. To verify this, we calculated energy histograms and cumulants for a number of different values of $K$. Figure 8 shows the results for the energy histograms near the corresponding critical temperatures (determined by the specific-heat peak locations) for $K = 0.1$ and $K = 5$. In contrast with the previous MC results for $K = 0$, a double-peak structure is not observed in the present cases indicative of a continuous phase transition.

The energy cumulant, defined by $U_E = 1 - \langle E^4 \rangle / 3 \langle E^2 \rangle^2$, was examined in Ref. 6 for $K = 0$ but provided inconclusive support for a first-order transition.[18] In the present work, this case is studied again along with an analysis of cumulant results at $K = 0.1$, 0.5, and 1 for lattice sizes $L = 18$, 24, 30, and 36. Simulations were performed at temperatures close to $T_N(L)$ estimated from specific-heat peaks using $10^6$ MCS. Figure 9 shows example data for the cases $K = 0$ and $K = 0.1$. The value of the minimum for each curve was estimated and clearly will depend on the temperature interval examined. Data collected for the study presented in Ref. 6 were at a relatively large interval of $\Delta T = 0.001$ whereas a smaller value of 0.0002 was used in the present work allowing for a more accurate estimate of the minima.
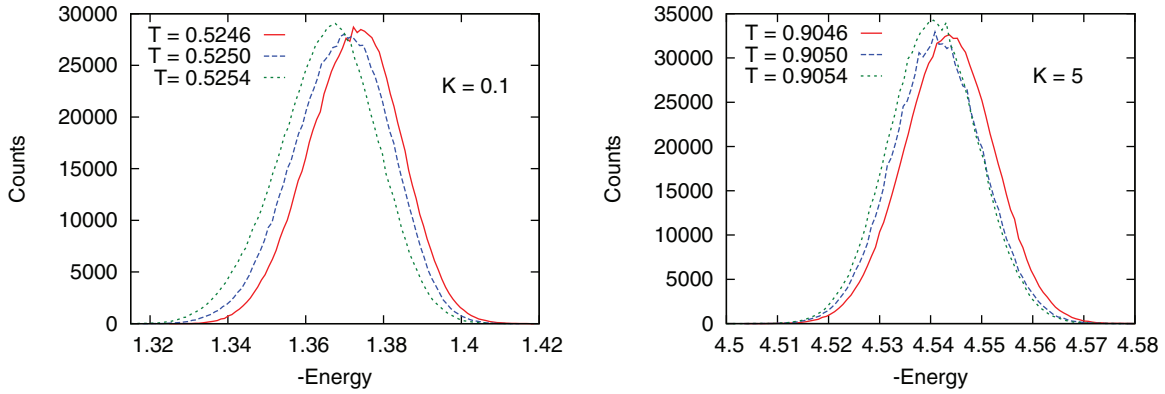
FIG. 8. (Color online) Energy histogram at values of $T$ near $T_N$ for $K = 0.1$ and $K = 5$ with $L = 36$ from simulations using $L = 24$.

Figure 10 shows our best estimation of the minima vs $1/N$ where $N$ is the number of magnetic lattice sites ($N = \frac{3}{4}L^3$) for $K = 0$, 0.1, 0.5, and 1. In the case of a continuous transition, the minimum should extrapolate to 2/3 in the thermodynamic limit.[18] Our data show a clear distinction in the trend of the finite-size scaling between the results for finite $K$, which appear to be consistent with the 2/3 limit, and the $K = 0$ case, in support of the notion that nonzero anisotropy drives the transition to be continuous.

## V. SUMMARY AND CONCLUSIONS

The extensive Monte Carlo simulations analyzed in this work have demonstrated the importance of cubic anisotropy on the ABC stacked kagome lattice of magnetic dipoles, relevant for fcc IrMn$_3$ and related compounds. An expression for the eight possible degenerate ground states is obtained at $T = 0$, allowing for an analytic description of the interspin angle showing an increasing deviation from 120° with increasing K. As a result of anisotropy, the spins develop a nonzero ferromagnetic moment along the [111] direction. Simulations show that the Néel temperature increases nonlinearly as the anisotropy strength is increased until a maximum at $K \simeq 5$ when it begins to overwhelm the exchange interaction. The transition temperature then decreases for larger $K$, approaching zero in the limit of infinite anisotropy. Additional simulations of the

present model to examine the interplay between anisotropy and an applied magnetic field have been initiated.[20]

It is argued that the large spin degeneracy of the pure isotropic Heisenberg model is removed with the addition of uniaxial anisotropy and that the phase transition to long-range $q = 0$, local 120°, magnetic order changes from first order[6] to continuous. Evidence to support this conjecture comes from simulation data on the energy histograms near $T_N$, which show a double peak[6] at $K = 0$ and a single peak at $K \neq 0$. Analysis of the Binder energy cumulant is also consistent with this conclusion. We speculate that the spin degeneracy of the pure Heisenberg model for this lattice leads to a first-order transition driven by order-by-disorder-type fluctuations. A preliminary analysis of the spin-wave modes in the 3D pure Heisenberg system show the presence of a zero-energy mode (for wave vectors along certain directions) which develops a finite energy of order $K$ as anisotropy is added.[8] It is anticipated that finite-temperature fluctuations remove the degeneracy associated with this $K = 0$ mode. A somewhat analogous effect has been shown to occur in the pyrochlore antiferromagnet Er$_2$Ti$_2$O$_7$ which involves a partial removal of the infinite ground-state degeneracy due to the addition of exchange anisotropy, leaving two separate spin states as basis functions for the 2D irreducible representation $E$ of the tetrahedral point group.[21] The present case is different in that the usual kagome degeneracy of spins
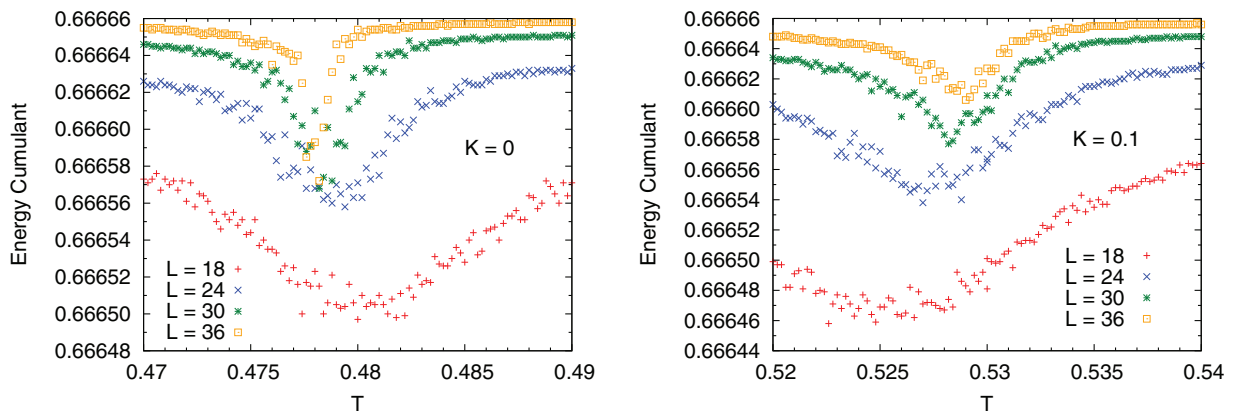


FIG. 9. (Color online) Energy cumulants for $K = 0$ and $K = 0.1$ at temperatures close to $T = T_N(L)$ estimated from the specific-heat peaks for the values of $L$ indicated.
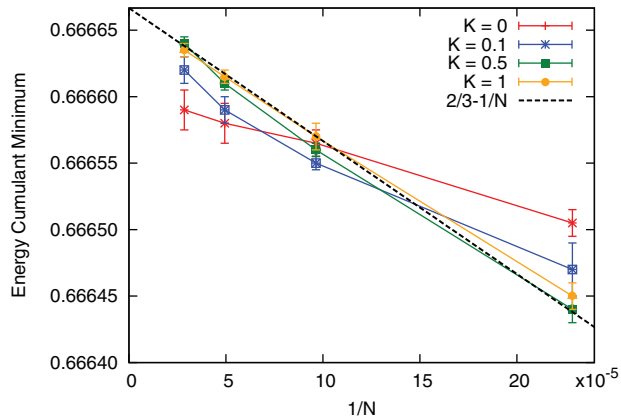
FIG. 10. (Color online) Estimated cumulant minima vs $1/N$ from the results of Fig. 9. Broken line shows behavior expected of a model continuous transition.

state with magnetic representation $2T_1 + T_2$ of the octahedral point group is fully removed.[22]

The development of a finite magnetic moment along the [111] direction as a consequence of anisotropy along with the expected in-plane canting of the spins on the top layer of the antiferromagnet in the presence of a ferromagnetic layer[17] are expected to be important to describe the exchange bias seen in $IrMn_3$. For this purpose, simulations are planned to study thin films of the fcc kagome structure and to also include exchange coupling to a ferromagnetic layer. Experimental verification of the presence of ferromagnetism in the bulk or thin-film ordered phase $IrMn_3$ and related compounds is desirable.

[1] A. B. Harris, C. Kallin, and A. J. Berlinsky, Phys. Rev. B **45**, 2899 (1992).

[2] M. E. Zhitomirsky, Phys. Rev. B **78**, 094423 (2008).

[3] G.-W. Chern and R. Moessner, Phys. Rev. Lett. **110**, 077201 (2013).

[4] P. Mendels and A. S. Wills, in *Introduction to Frustrated Magnetism*, edited by C. Lacroix, P. Mendels, and F. Mila, Springer Series in Solid-State Sciences Vol. 164 (Springer, Heidelberg, 2011).

[5] L. Szunyogh, B. Lazarovits, L. Udvardi, J. Jackson, and U. Nowak, Phys. Rev. B **79**, 020403 (2009).

[6] V. Hemmati, M. L. Plumer, J. P. Whitehead, and B. W. Southern, Phys. Rev. B **86**, 104419 (2012).

[7] K. Marty, V. Simonet, E. Ressouche, R. Ballou, P. Lejay, and P. Bordet, Phys. Rev. Lett. **101**, 247201 (2008).

[8] M. D. Leblanc and B. W. Southern (unpublished).

[9] M. Tsunoda, H. Takahashi, and M. Takahashi, IEEE Trans. Magn. **45**, 3877 (2009).

[10] M. Tsunoda, H. Takahashi, T. Nakamura, C. Mitsumata, S. Isogami, and M. Takahashi, Appl. Phys. Lett. **97**, 072501 (2010).

[11] L. Szunyogh, L. Udvardi, J. Jackson, U. Nowak, and R. Chantrell, Phys. Rev. B **83**, 024401 (2011).

[12] E. Krén, G. Kádár, L. Pál, J. Sólyom, and P. Szabó, Phys. Lett. **20**, 331 (1966); E. Krén, G. Kádár, L. Pál, J. Sólyom, P. Szabó, and T. Tarnóczi, Phys. Rev. **171**, 574 (1968); A. Sakuma, R. Y. Umetsu, and K. Fukamichi, Phys. Rev. B **66**, 014432 (2002); T. Ikeda and Y. Tsunoda, J. Phys. Soc. Jpn. **72**, 2614 (2003).

[13] I. Tomeno, H. N. Fuke, H. Iwasaki, M. Sahashi, and Y. Tsunoda, J. Appl. Phys. **86**, 3853 (1999).

[14] K. O'Grady, L. E. Fernandez-Outon, and G. Vallejo-Fernandez, J. Magn. Magn. Mater. **322**, 883 (2010).

[15] H. Takahashi, Y. Kota, T. Tsunoda, K. Kodama, A. Sakuma, and M. Takahashi, J. Appl. Phys. **110**, 123920 (2011).

[16] H. Takahashi, M. Tsunoda, and M. Takahashi, IEEE Trans. Magn. **48**, 4347 (2012).

[17] B.-Y. Wang, J.-Y. Hong, K.-H. O. Yang, Y.-L. Chan, D.-H. Wei, H.-J. Lin, and M.-T. Lin, Phys. Rev. Lett. **110**, 117203 (2013).

[18] M. S. S. Challa, D. P. Landau, and K. Binder, Phys. Rev. B **34**, 1841 (1986).

[19] F. G. West, J. Appl. Phys. **32**, 249S (1961).

[20] B. W. Southern (unpublished).

[21] M. E. Zhitomirsky, M. V. Gvozdikova, P. C. W. Holdsworth, and R. Moessner, Phys. Rev. Lett. **109**, 077204 (2012).

[22] M. Tinkham, *Group Theory and Quantum Mechanics* (McGraw-Hill, New York, 1964).